Articles

Crystal Structure of the Ephrin-B1 Ectodomain: Implications for Receptor Recognition and Signaling†

Dimitar B. Nikolov, Chen Li, William A. Barton,‡ and Juha-Pekka Himanen*

Structural Biology Program, Memorial Sloan-Kettering Cancer Center, New York, New York 10021

Received April 28, 2005; Revised Manuscript Received June 23, 2005

ABSTRACT: Eph receptors and their ephrin ligands are involved in various aspects of cell−cell communication during development, including axonal pathfinding in the nervous system and cell−cell interactions of the vascular endothelial cells. Recent structural studies revealed unique molecular features, not previously seen in any other receptor−ligand families, and explained many of the biochemical and signaling properties of Ephs and ephrins. However, unresolved questions remain regarding the potential oligomerization and clustering of these important signaling molecules. In this study, the biophysical properties and receptor-binding preferences of the extracellular domain of ephrin-B1 were investigated and its crystal structure was determined at 2.65 Å resolution. Ephrin-B1 is a monomer both in solution and in the crystals, while it was previously shown that the closely related ephrin-B2 forms homodimers. The main structural difference between ephrin-B1 and ephrin-B2 is the conformation of the receptor-binding G−H loop and the partially disordered N-terminal tetramerization region of ephrin-B1. The G−H loop is structurally rigid in ephrin-B2 and adopts the same conformation in both the receptor-bound and unbound ligand, where it mediates receptor-independent homodimerization. In the ephrin-B1 structure, on the other hand, the G−H loop is not involved in any homotypic interactions and adopts a new, distinct conformation. The implications of the ephrin-B1 structure, in context of available ephrin-B1 mutagenesis data, for the mechanism of Eph−ephrin recognition and signaling initiation are discussed.

The Eph receptor tyrosine kinases (Ephs) and their ephrin ligands are involved in various regulatory events of embryonic tissue morphogenesis and development. They also have well-defined roles in the function of many tissues and organs of the adult body, including regulating nervous system plasticity and blood vessel integrity (*1*, *2*). The involvement of Eph receptors and ephrins in cancer formation and progression is also now well-established (*3*−*7*). Recently, ephrin-B1 was shown also to be involved in T-cell activation (*8*), platelet aggregation (*9*), and morphogenetic movements of cells during development (*10*, *11*).

The Ephs and the ephrins are divided into two subclasses, A and B, based on their affinities for each other and on sequence conservation (*12*). In general, the 10 different EphA receptor tyrosine kinases (EphA1−A10) promiscuously bind to and are activated by six A ephrins (ephrin-A1−A6) that are attached to the cell via a glycosylphosphatidylinositol (GPI) linkage. The EphB subclass receptors (EphB1−B6) interact with three different B ephrins (ephrin-B1−B3) that are attached to the cell by a hydrophobic transmembrane region and a short cytoplasmic domain (*13*). Because not only the receptors but also the ligands are membrane-attached, their interaction occurs only at sites of cell−cell contact. This leads to a multimerization of both molecules to distinct clusters within their respective plasma membranes and results in the initiation of a bidirectional signaling (forward signaling in the Eph receptor-expressing cell and reverse signaling in the ephrin-expressing cell), characteristic to this group of molecules (*14*, *15*).

The extracellular region of Eph receptors contains a highly conserved N-terminal ligand-binding domain. An immediately adjacent cysteine-rich region may be involved in receptor−receptor oligomerization often observed upon ligand binding (*16*), while the following two fibronectin repeats are yet to be assigned a clear biological function. The cytoplasmic region of Eph receptors contains a highly conserved kinase domain (*17*), a sterile α motif (SAM)[1] domain, and a PDZ-binding motif. All ephrins contain a 20-kDa conserved extracellular receptor-binding domain. B-type ephrins also possess a short cytoplasmic region that becomes phosphorylated upon receptor binding, thus initiating a reverse signaling cascade. A C-terminal PDZ-binding

† This work was financially supported by the NIH (R01-NS38486). The atomic coordinates have been deposited in the Protein Data Bank.

* To whom correspondence should be addressed: Memorial Sloan-Kettering Cancer Center, 1275 York Avenue, Box 297, New York, NY 10021. Telephone: (212) 639-6837. Fax: (212) 717-3135. E-mail: himanenj@mskcc.org.

‡ Present address: Institute for Structural Biology and Drug Discovery, Virginia Commonwealth University, Richmond, VA 23219.

[1] Abbreviations: HEK, human embryonic kidney; GPI, glycosylphosphatidylinositol; SAM, sterile α motif; FRET, fluorescence resonance energy transfer; CFNS, craniofrontonasal syndrome.

10.1021/bi050789w CCC: $30.25
Published on Web 07/30/2005

motif is involved in protein interactions mediating membrane localization and reverse signaling (*18*).

In our earlier biochemical and crystallographic studies, we determined the crystal structures of the EphB2/ephrin-B2 and EphB2/ephrin-A5 complexes (*19*, *20*). We demonstrated that interaction domains of EphB2 and ephrin-B2 initially form high-affinity heterodimers that can then further associate, with a lower K_d, to form 2:2 heterotetramers (*15*, *21*). The high-affinity interface, responsible for the initial 1:1 binding is very extensive and centers around the G−H loop of the ligand that penetrates deep into a channel on the surface of the receptor. Interestingly, in a separate study describing the structure of unligated ephrin-B2 (the only reported structure thus far of an unligated ephrin), this loop was found to be involved in the formation of ligand dimers in the absence of the receptor (*22*). The authors further proposed that the ephrin-B2 dimer present in the crystal could be an activating species *in vivo*. The reported ephrin-B2 dimerization raises important questions about whether other ephrins could also participate in receptor-independent homodimerization interactions and how these dimers could affect the Eph-mediated signaling initiation. Because in the EphB2/ephrin-B2 complex structure the same ephrin surface is directly involved in receptor recognition, the "incoming" EphB2 receptor on the surface of a cell would have to replace one of the ephrin-B2 molecules in a ligand dimer to form a signaling-competent complex. This observation calls for further studies with other ephrin family members on the oligomerization state of the unbound ligands and the molecular details of the ligand/receptor interactions. We, therefore, have determined and report here the crystal structure of another EphB2-specific ligand, ephrin-B1.

EXPERIMENTAL PROCEDURES

Protein Expression. The extracellular, receptor-binding domain of murine ephrin-B1 (residues Thr-26−Arg-198) was expressed as an Fc-fusion protein in a HEK293 (human embryonic kidney) cell line using a CD5 signal sequence essentially as described in ref *23*. The protein was purified by protein-A Sepharose affinity and Superdex 200 size-exclusion chromatography using Akta Explorer chromatographic system (Amersham), and the Fc tag was removed by thrombin cleavage. Extracellular domains of ephrin-B2 and EphB4 were expressed using the same HEK293 system. The murine EphB2 globular domain (residues 28−210) was expressed using the pET32 vector and *Escherichia coli* strain AD494(DE3) (Novagen) as described in ref *24*.

Pull-Down Experiments. Pull-down experiments were performed as described earlier (*24*). In brief, 5 μg of the recombinant receptor-binding domain of ephrin-B1 was incubated with Fc-tagged Eph ectodomains (R&D Systems) at room temperature for 30 min in 500 μL binding buffer containing 20 mM HEPES (pH 8.2), 150 mM KCl, and 2 mM $MgCl_2$. Protein-A Sepharose Fast Flow beads (Amersham) were washed with the binding buffer, added to the reaction mixture, and shaken at room temperature for 30 min. The beads were then harvested by centrifugation and washed twice with 500 μL of the binding buffer, and the bound proteins were separated on a 10−20% polyacrylamide gel.

Fluorometry and Ultracentrifugation. Eph−ephrin binding constants were measured by HTRF technology (Cisbio) with Eu^{3+} cryptate and XL665 as donor and acceptor labels, respectively. When the interaction between the Fc-labeled receptor and ligand brings the labels into close proximity, FRET (fluorescence resonance energy transfer) occurs upon excitation at 620 nm with XL665 re-emitting a specific long-lived fluorescence at 665 nm. An increasing amount of ephrin−Fc gives an increasing FRET signal until a plateau is reached, and binding constants can be calculated using "KaleidaGraph" software. Measurements were done in 384-well plates (Falcon). The total reaction volume was 20 μL. The concentration of the labeled Eph−Fc was kept at a constant 50 nM in a 100 mM Na-phosphate buffer (pH 7.0) and 200 mM Na-fluoride. The concentration of the labeled ephrin−Fc varied typically between 10 and 200 nM. Concentrations of the labels were according to the recommendations of the manufacturer. Analytical ultracentrifugation was performed on a Beckman XL-A centrifuge equipped with an An-60 Ti rotor. Protein solution was loaded at a concentration of 30 μM in 10 mM HEPES at pH 7.5 and 0.4 M KCl and analyzed at a rotor speed of 11 krpm at 20 °C (*16*), and the molecular weight was calculated using the method described in ref *25*.

Table 1: Summary of Crystallographic Analysis

resolution (Å)	2.65
wavelength (Å)	0.98
completeness (%)	97.1 (96.9)
redundancy (fold)	4.2
$I/\sigma I$	12.0 (3.2)
R_{sym} (%)	9.0 (38.5)
space group	$P2_1$
cell dimensions (Å)	$a = 48.716$, $b = 29.682$, $c = 56.268$ $\beta = 100.509°$
refinement	
resolution (Å)	2.65
reflections working/test	4439/210
residues	139
ligands	1 *N*-acetyl glucosamine
R_{crys}/R_{free}	27.1/30.0 (26.1/36.8)
rmsd values	
bonds (Å)	0.010
angles (deg)	1.273
average *B* factor (Å^2)	36.6
Ramachandran analysis	
most favored (%)	74.4
additionally allowed (%)	22.2
generously allowed (%)	3.4
disallowed (%)	0.0

Crystallization and Data Collection. The purified ephrin-B1 was concentrated to 20 mg/mL and crystallized in a hanging drop at 25 °C against the reservoir containing 30% (w/v) polyethylene glycol 8000, 200 mM ammonium sulfate, 100 mM Na-cacodylate at pH 6.5, and 4% (v/v) 1,3-propanediol (Hampton Research). Data were collected at the NSLS Brookhaven beamline X9A and CHESS beamline A1. Images were integrated, scaled, and merged using DENZO and SCALEPACK (*26*, *27*). The structure of the ephrin-B1 was determined using molecular replacement with the CCP4 program Amore and Refmac (*28*) and the ephrin-B2 structure (PDB 1KGY) as a search model. The structure was refined by rigid-body refinement, followed by an iterative process of model improvement in O (*26*) and Cartesian molecular dynamics and energy minimization refinement in CNS (*29*; see Table 1).

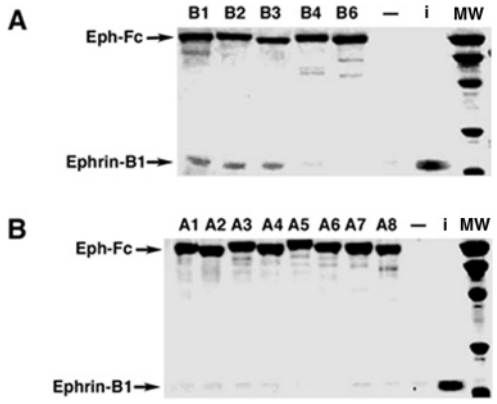

FIGURE 1: Binding of ephrin-B1 to EphB or EphA receptors. The extracellular, receptor-binding domain of murine ephrin-B1 (residues Thr-26−Arg-198) was expressed in a HEK293 cell line, purified by protein-A Sepharose affinity and Superdex 200 size-exclusion chromatography, and the Fc tag was removed by thrombin cleavage. Pull-down experiments were done using commercial Fc-tagged receptors and protein-A Sepharose beads. The bound proteins were separated on a 10−20% polyacrylamide gel. Ephrin-B1 binds strongly to EphB1, EphB2, and EphB3 and weakly to EphB4 but does not bind to EphB6 (A) or any of the A-class Eph receptors (B). A dash (—) indicates a control experiment where ephrin-B1 was incubated with protein-A beads alone, without any of the Fc-tagged receptors. Lane "i" stands for "input", where ephrin-B1 was loaded directly on the gel, without being pulled-down. Molecular weight markers (labeled "MW") are, from top to bottom, 97.4, 66.2, 45.0, 31.0, and 21.5 kDa.

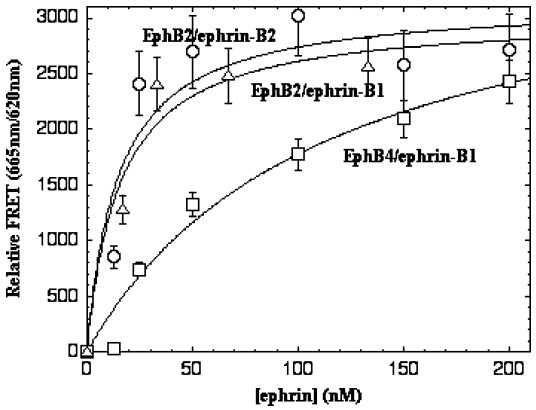

FIGURE 2: Fluorometric measurement of ephrin binding to EphB2 or EphB4. Measurements were done by FRET-based HTRF technology as described in the Experimental Procedures. The dissociation constant (K_d) of 12 nM for ephrin-B1 binding to EphB2 is slightly higher than that for ephrin-B2 (4 nM), the preferred high-affinity ligand of EphB2 (*12*), while the binding of ephrin-B1 to EphB4 has a dramatically higher K_d value (112 nM). ○ corresponds to EphB2/ephrin-B2; △ corresponds to EphB2/ephrin-B1; and □ corresponds to EphB4/ephrin-B1.

RESULTS AND DISCUSSION

Receptor-Binding Preferences of Ephrin-B1. To confirm the biological activity of the purified recombinant ephrin-B1, we evaluated its binding to several A- and B-class Eph receptors. In pull-down experiments (parts A and B of Figure 1) using Fc-tagged extracellular domains of Eph receptors, ephrin-B1 showed strong binding to EphB1, EphB2, and EphB3, weak binding to EphB4, and no binding to EphB6 or any of the A-class Eph receptors. This finding is in agreement with previous cell-based binding and signaling-activation studies aimed at characterizing the biological properties of ephrin-B1 (*30*). Analysis of the available Eph sequences suggest that the drastically weaker binding of ephrin-B1 to EphB4 or EphB6 could be explained by the fact that EphB4 and EphB6 have a three amino acid insertion in their J−K loop that forms part of the channel on the surface of the receptor (*19*, *20*). This channel is crucial for the initial high-affinity ligand−receptor heterodimerization, and the insertion is likely to affect the ephrin−Eph recognition.

We also used fluorophore labeling (FRET) to measure the binding affinities of ephrin-B1 and ephrin-B2 to EphB2. The observed apparent dissociation constant of 12 nM (Figure 2) for ephrin-B1 is slightly higher than that observed for ephrin-B2 (K_d = 4 nM), the preferred high-affinity ligand of EphB2 (*12*). Consistent with the pull-down experiments, ephrin-B1 shows in the fluorescence assay a considerably lower binding affinity to EphB4 than to EphB2 with an apparent K_d of 112 nM (Figure 2).

Ephrin-B1 Is a Monomer in Solution. Analytical ultracentrifugation was used to determine the oligomeric state of ephrin-B1. As shown in Figure 3A, the purified ephrin-B1 (at 30 μM concentration) is monomeric with an apparent molecular weight of 21 kDa, well in agreement with the theoretical value of 19 379 Da (ephrin-B1 amino acids 26−198) with the difference likely because of glycosylation.

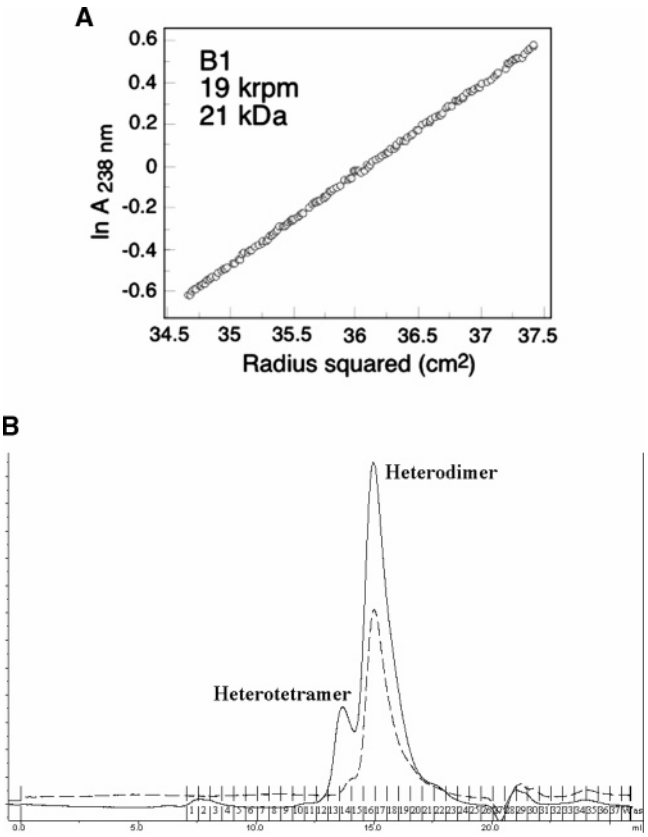

FIGURE 3: (A) Determination of molecular weight of ephrin-B1 by analytical ultracentrifugation analysis. Using the methods described in ref *25*, ephrin-B1 was calculated to have a molecular weight of 21 kDa corresponding to a monomer. (B) Superdex-200 size-exclusion chromatography elution profiles of ephrin-B1 (···) or ephrin-B2 (—) both in complex with EphB2. Purified protein complexes were concentrated to ~300 μM and run at 0.5 mL/min in the presence of 20 mM HEPES (pH 7.2) and 500 mM KCl. The presence of the ephrin−Eph complex in the peaks was confirmed by SDS gel electrophoresis. While ephrin-B2 forms both heterodimers and heterotetramers with EphB2, ephrin-B1 forms mostly heterodimers.

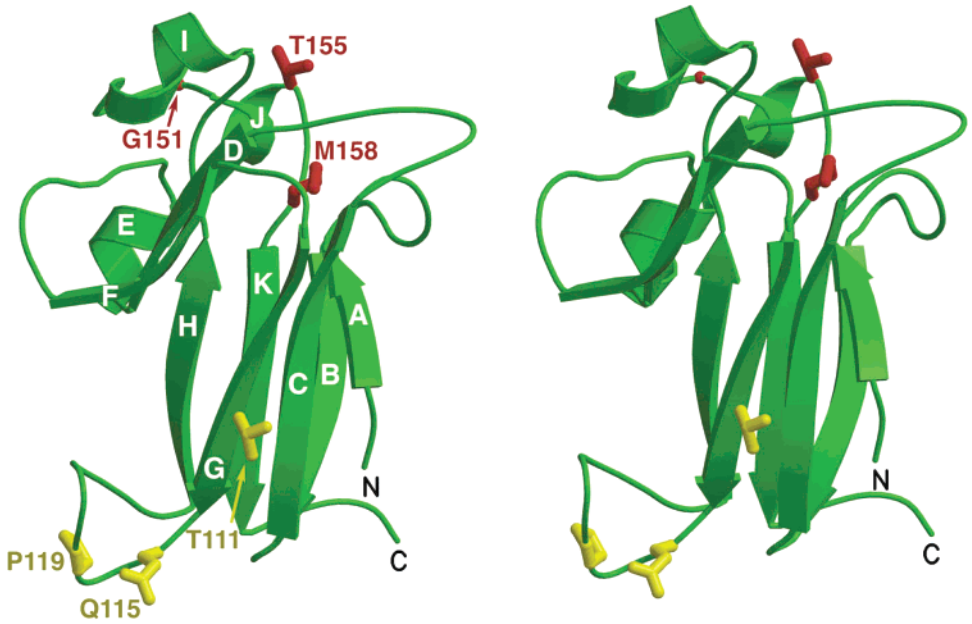

FIGURE 4: Crystal structure of ephrin-B1. Crystals of the purified ephrin-B1 were obtained as described in the text, and the structure was determined using molecular replacement with ephrin-B2 as a search model. Shown is a stereoview of the ephrin-B1 structure highlighting the six surface-exposed point mutations that cause CFNS. Three of these mutants, colored in yellow, map to (or close to) the dimerization G−H loop, and the other three, colored in red, map to the J−K region that is not involved in either dimerization or tetramerization interactions in the ephrin-B2/EphB2 complex.

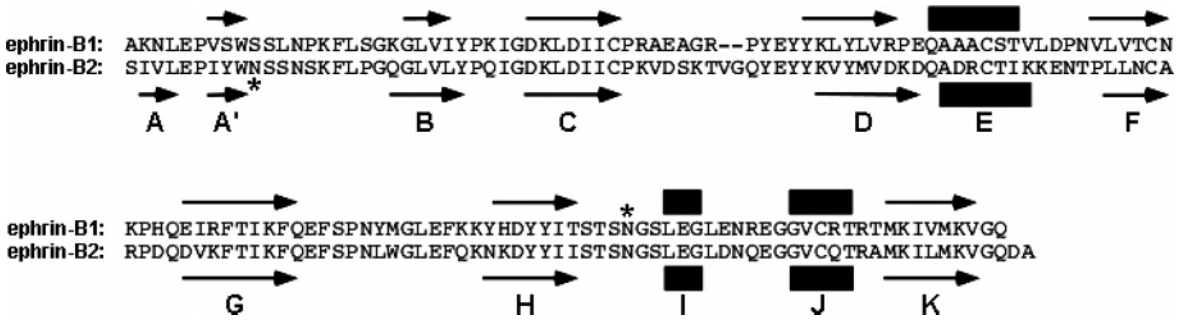

FIGURE 5: Sequence alignment of ephrin-B1 and ephrin-B2. The two sequences have 43% amino acid identity. Secondary structure elements are shown as arrows for β strands and as rectangles for helices. The positions of *N*-acetyl-glucosamine moieties are indicated with asterisks.

Ephrin-B1 also migrates as a monomer during gel-filtration chromatography (data not shown).

Interestingly, on a size-exclusion column, the EphB2/ephrin-B1 complex has an elution profile different to that of the EphB2/ephrin-B2 complex. While the EphB2/ephrin-B2 complex has two clearly separated peaks, one corresponding to the 1:1 heterodimeric complex (15.0 mL) and the other to the 2:2 heterotetrameric complex (13.6 mL) (Figure 3B; see also ref *21*), the EphB2/ephrin-B1 complex runs mostly as a heterodimer even at high concentrations (300 μM).

Crystal Structure of Ephrin-B1. Ephrin-B1 was concentrated to 20 mg/mL and crystallized in a hanging drop at room temperature against a reservoir containing 30% (w/v) polyethylene glycol 8000, 200 mM ammonium sulfate, 100 mM Na-cacodylate at pH 6.5, and 4% (v/v) 1,3-propanediol (Hampton Research). Crystals grew in the $P2_1$ space group (a = 48.716, b = 29.682, c = 56.268, and β = 100.509°), with one molecule in the asymmetric unit. The structure was determined at 2.65 Å resolution using molecular replacement and the ephrin-B2 structure as a search model and refined to a crystallographic R_{factor} of 27% and R_{free} of 30%. The statistics of crystallographic data are summarized in Table 1.

The folding topology of the ephrin-B1 ectodomain (Figure 4) is a variation of the common Greek key β barrel with eight mixed parallel and antiparallel β strands forming two β sheets around a hydrophobic core and three α helices connecting the strands. Two buried disulfide bonds stabilize the structure. Ephrin-B1 shares significant sequence homology (43% amino acid identity) with ephrin-B2. Figure 5 shows the sequence alignment and the organization of secondary structure elements of ephrin-B1 and ephrin-B2. As expected from their sequence homology, the overall structure of ephrin-B1 is very similar to that of ephrin-B2 (*19*, *22*), and the two structures can be superimposed with root-mean-square deviations (rmsd values) between 126 equivalent α-carbon positions of 1.1 Å (Figure 6).

Ephrin-B1 Receptor-Binding Loop Adopts a Unique Conformation. The most structurally distinct region of ephrin-B1 is in the receptor-binding (G−H) loop (*19*). It has an extended but at the same time quite rigid structure in ephrin-B2, where it is also involved in ephrin homodimerization (*22*). In ephrin-B1, on the other hand, it is not involved in

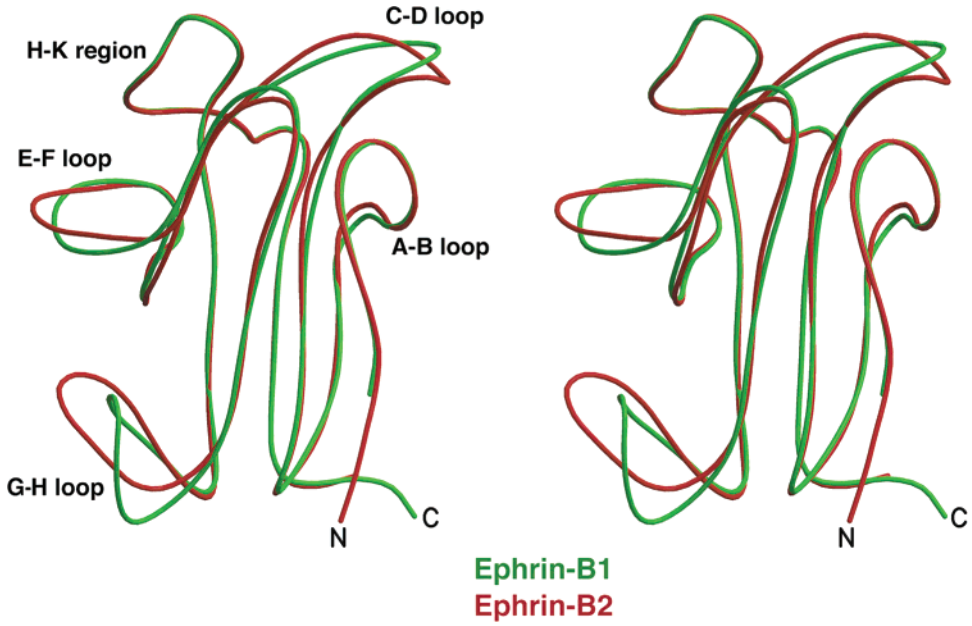

FIGURE 6: Superimposition of the structures of ephrin-B1 (green) and ephrin-B2 (red). The rmsd between the corresponding Cα positions is 1.1 Å. The most structurally distinct region of ephrin-B1 is the receptor-binding (G−H) loop in the dimerization interface that is more flexible than in ephrin-B2 and is not involved in the formation of ligand homodimers. In addition, the N-terminal A β strand (which is important for Eph/ephrin tetramerization) of ephrin-B1 is unstructured and was not build in the model.

ephrin−ephrin interactions in the crystal lattice (Figure 6) and is structurally more flexible. Indeed, while the average *B* factor for ephrin-B1 is 35, the G−H loop has an average *B* factor of 45 (maximal *B* factor of 60). The distinct conformation of the G−H loop in the unbound ephrin-B1 suggests that it undergoes structural readjustment to obtain the Eph-channel-binding conformation required for high-affinity Eph/ephrin complex formation (*19*) and recognizes its cognate Eph receptors via an induced fit mechanism, where both the ligand and the receptor undergo conformational changes upon complex formation.

The flexibility of the G−H loop further suggests that longer and more flexible peptides could be identified that could potentially bind in the Eph surface channel and function as antagonists of the Eph-mediated signaling. Following this line of reasoning, it is interesting to note that in two separate studies Pasquale's group used phage display to identify peptides that bind Eph receptors with high affinity (submicromolar K_d values) and antagonize ephrin signaling (*31*, *32*). It is likely that these peptides that share only moderate sequence homology with the G−H ephrin loop follow a similar "induced fit" mechanism of interacting with the ligand-binding surface channel of the Eph receptors.

Partially Disordered N Terminus of Ephrin-B1 Reduces Heterotetramer Stability. Another interesting difference between the structures of ephrin-B1 and ephrin-B2 is the partial disorder of the N-terminal ephrin-B1 region, where the residues, corresponding to β strand "A" of ephrin-B2 (Figure 5), are not visible in the electron density. In our earlier studies (*19*), we have shown that the ephrin-B2/EphB2 tetramerization (or "low-affinity") interface has two distinct regions. The one involving the N-terminal A and A′ strands of ephrin-B2 contains most of the ligand−receptor contacts. A partial disordering in this ephrin region could, therefore, negatively affect the formation of functional ligand/receptor heterotetramers. Furthermore, in the EphB2/ephrin-B2 structure, the aromatic rings of Tyr-37 of ephrin-B2 and Phe-128 of EphB2 stack against each other, and the substitution of Tyr-37 for Ser in ephrin-B1 is likely to further destabilize the ephrin-B1/EphB2 heterotetramer.

We have previously shown that the unorthodox (cross-class) ephrin-A5/EphB2 complex crystallizes as a heterodimer (*20*). It is interesting to note that the EphB2-bound ephrin-A5 has an N terminus that is also structurally distinct from that of ephrin-B2. Instead of a rigid β strand, the N terminus of ephrin-A5 forms a "kink" protruding away from the core of the structure. This, together with the four amino acid insertion in the class specificity Eph H−I loop (*24*) (which interacts with the ephrin N terminus) in B-class receptors, renders ephrin-A5 entirely unable to form the heterotetrameric complex with the ligand-binding domain of EphB2. It is well-conceivable, on the other hand, that ephrin-B1, which is a B-class ligand and favors B-class receptors containing longer H−I loops, will form functional heterotetramers with EphB2 at high protein concentrations, such as the ones observed at interacting cell surfaces or in a crystal.

Ephrin-B1 is glycosylated, and an *N*-acetyl-glucosamine moiety attached to Asn-139 (Figure 5) was identified in the electron-density map and included in the final model. Interestingly, ephrin-B2 is glycosylated not at Asn-139 but at Asn-39 (*22*), which is immediately adjacent to the important heterotatramerization Eph/ephrin interface (*19*). It has been speculated that the Asn-39 glycosylation might modulate/enhance the Eph/ephrin interactions, and the fact that ephrin-B1 lacks the modification at this position could further explain its lower binding affinity to EphB2 as compared to ephrin-B2 (Figure 2) and its reduced tendency to form heterotetramers with the ligand-binding domain of EphB2 (Figure 3B).

Implications for the Formation of Signaling-Competent Complexes. While the structural and biophysical experiments in this study reveal details about the initial recognition and binding of ephrin-B1 to EphB2, the molecular interfaces mediating the higher-order Eph/ephrin cluster formation

(which are required for efficient signaling; *33*) still remain elusive. Several recent findings shed some light on this question. First, it was shown that point mutations in the ephrin-B1 gene cause X-chromosome-linked craniofrontonasal syndrome (CFNS) where the affected individuals exhibit craniofacial abnormalities, such as orbital asymmetry (*34*, *35*). Six of these mutants cause changes in surface-exposed amino acids of ephrin-B1 (and are thus unlikely to result in unstable or inactive proteins). As shown in Figure 4, three mutants (at ephrin-B1 positions 111, 115, and 119) map to the G−H loop at the high-affinity Eph/ephrin interface, while the other three (positions 151, 155, and 158) map to the J−K region that is not involved in any ligand−receptor interactions observed in the structure of the ephrin-B2/EphB2 complex (*19*). The importance of this latter ephrin surface region for causing CFNS suggests that it might be involved in the formation of higher-order ligand−receptor clusters at the cites of cell−cell contact. This concept gets further support from two studies (*23*, *36*) in which random mutagenesis was used to identify EphA3 and ephrin-A5 surfaces essential for ligand−receptor recognition and signaling. The identified areas include not only the structurally characterized heterodimerization and heterotetramerization interfaces but also part of the EphA3 cysteine-rich linker (which was not included in the structural studies), as well as a small ephrin-A5 surface region that includes the structural elements harboring the CFNS mutations in ephrin-B1.

In conclusion, our structural and biophysical studies document that ephrin-B1 is a monomer in a wide concentration range (from 30 to 300 μM) and its G−H loop is not involved in receptor-independent homodimerization interactions, such as the ones reported for ephrin-B2 (*22*). The G−H loop of ephrins might thus be involved in fine tuning of the Eph−ephrin signaling where some (such as the high-affinity EphB2 ligand, ephrin-B2) but not all ligands induce a faster and stronger signal because they exist as predimerized entities on the surface of the cell. To obtain further insight into these questions, structural and biophysical studies are also necessary on A-class ephrins and A-class Eph/ephrin complexes.

ACKNOWLEDGMENT

We thank Dr. Min Lu for performing the analytical ultracentrifugation experiment. We are grateful to the staff at the NSLS and CHESS synchrotrons for their help with data collection.

REFERENCES

1. Wang, H. U., Chen, Z. F., and Anderson, D. J. (1998) Molecular distinction and angiogenic interaction between embryonic arteries and veins revealed by ephrin-B2 and its receptor Eph-B4, *Cell 93*, 741−753.
2. Kullander, K., and Klein, R. (2002) Mechanism and function of Eph and ephrin signaling, *Nat. Rev. Mol. Cell Biol. 3*, 475−486.
3. Dodelet, V. C., and Pasquale, E. B. (2000) Eph receptors and ephrin ligands: Embryogenesis to tumorigenesis, *Oncogene 19*, 5614−5619.
4. Andres, A. C., Reid, H. H., Zurcher, G., Blaschke, R. J., Albrecht, D., and Ziemiecki, A. (1994) Expression of two novel eph-related receptor protein tyrosine kinases in mammary gland development and carcinogenesis, *Oncogene 9*, 1461−1467.
5. Kao, H. W., Chen, H. C., Wu, C. W., and Lin, W. C. (2003) Tyrosine-kinase expression profiles in human gastric cancer cell lines and their modulations with retinoic acids, *Br. J. Cancer 88*, 1058−1064.
6. Adams, R. H., Wilkinson, G. A., Weiss, C., Diella, F., Gale, N. W., Deutsch, U., Risau, W., and Klein, R. (1999) Roles of ephrinB ligands and EphB receptors in cardiovascular development: Demarcation of arterial/venous domains, vascular morphogenesis, and sprouting angiogenesis, *Genes Dev. 13*, 295−306.
7. Bennett, B. D., Wang, Z., Kuang, W. J., Wang, A., Groopman, J. E., Goeddel, D. V., and Scadden, D. T. (1994) Cloning and characterization of HTK, a novel transmembrane tyrosine kinase of the EPH subfamily, *J. Biol. Chem. 269*, 14211−14218.
8. Yu, G., Luo, H., Wu, Y., and Wu J. (2004) EphrinB1 is essential in T-cell-T-cell co-operation during T-cell activation, *J. Biol. Chem. 279*, 55531−55539.
9. Prevost, N., Woulfe, D. S., Tognolini, M., Tanaka, T., Jian, W., Fortna, R. R., Jiang, H., and Brass, L. F. (2004) Signaling by ephrinB1 and Eph kinases in platelets promotes Rap1 activation, platelet adhesion, and aggregation via effector pathways that do not require phosphorylation of ephrinB1, *Blood 103*, 1348−1355.
10. Compagni, A., Logan, M., Klein, R., and Adams, R. H. (2003) Control of skeletal patterning by ephrinB1−EphB interactions, *Dev. Cell 5*, 217−230.
11. Moore, K. B., Mood, K., Daar, I. O., and Moody, S. A. (2004) Morphogenetic movements underlying eye field formation require interactions between the FGF and ephrinB1 signaling pathways, *Dev. Cell 6*, 55−67.
12. Gale, N. W., Holland, S. J., Valenzuela, D. M., Flenniken, A., Pan, L., Ryan, T. E., Henkemeyer, M., Strebhardt, K., Hirai, H., Wilkinson, D. G., Pawson, T., Davis, S., and Yancopoulos, G. D. (1996) Eph receptors and ligands comprise two major specificity subclasses and are reciprocally compartmentalized during embryogenesis, *Neuron 17*, 9−19.
13. Klein, R. (2001) Excitatory Eph receptors and adhesive ephrin ligands, *Curr. Opin. Cell Biol. 13*, 196−203.
14. Henkemeyer, M., Marengere, L. E., McGlade, J., Olivier, J. P., Conlon, R. A., Holmyard, D. P., Letwin, K., and Pawson, T. (1994) Immunolocalization of the Nuk receptor tyrosine kinase suggests roles in segmental patterning of the brain and axonogenesis, *Oncogene 9*, 1001−1014.
15. Himanen, J. P., and Nikolov, D. B. (2003) Eph signaling: A structural view, *Trends Neurosci. 26*, 46−51.
16. Lackmann, M., Mann, R. J., Kravets, L., Smith, F. M., Bucci, T. A., Maxwell, K. F., Howlett, G. J., Olsson, J. E., Vanden Bos, T., Cerretti, D. P., and Boyd, A. W. (1997) Ligand for EPH-related kinase (LERK) 7 is the preferred high affinity ligand for the HEK receptor, *J. Biol. Chem. 272*, 16521−16530.
17. Hubbard, S. R., and Till, J. H. (2000) Protein tyrosine kinase structure and function, *Annu. Rev. Biochem. 69*, 373−398.
18. Cowan, C. A., and Henkemeyer, M. (2001) The SH2/SH3 domain adaptor Grb4 transduces B-ephrin reverse signals, *Nature 413*, 174−179.
19. Himanen, J. P., Rajashankar, K. R., Lackmann, M., Cowan, C. A., Henkemeyer, M., and Nikolov, D. B. (2001) Crystal structure of an Eph receptor−ephrin complex, *Nature 414*, 933−938.
20. Himanen, J. P., Chumley, M. J., Lackmann, M., Li, C., Barton, W. A., Jeffrey, P. D., Vearing, C., Geleick, D., Feldheim, D. A., Boyd, A. W., Henkemeyer, M., and Nikolov, D. B. (2004) Repelling class discrimination: Ephrin-A5 binds to and activates EphB2 receptor signaling, *Nat. Neurosci. 7*, 501−509.
21. Himanen, J. P., and Nikolov, D. B. (2002) Purification, crystallization, and preliminary characterization of an Eph-B2/ephrin-B2 complex, *Acta Crystallogr., Sect. D: Biol. Crystallogr. 58*, 533−535.
22. Toth, J., Cutforth, T., Gelinas, A. D., Bethoney, K. A., Bard, J., and Harrison, C. J. (2001) Crystal structure of an ephrin ectodomain, *Dev. Cell 1*, 83−92.
23. Smith, F. M., Vearing, C., Lackmann, M., Treutlein, H., Himanen, J., Chen, K., Saul, A., Nikolov, D., and Boyd, A. W. (2004) Dissecting the EphA3/ephrin-A5 interactions using a novel functional mutagenesis screen, *J. Biol. Chem. 279*, 9522−9531.
24. Himanen, J. P, Henkemeyer, M., and Nikolov, D. B. (1998) Crystal structure of the ligand-binding domain of the receptor tyrosine kinase EphB2, *Nature 396*, 486-491.
25. Brenner, S. L., Zlotnick, A., and Stafford, W. F. I. (1993) RecA protein self-assembly II. Analytical equilibrium ultracentrifucation studies of the entropy-driven self-association of RecA, *J. Mol. Biol. 216*, 949−964.
26. Jones, T. A., Zou, J. Y., Cowan, S. W., and Kjeldgaard, M. (1991) Improved methods for building protein models in electron density maps and the location of errors in these models, *Acta Crystallogr., Sect. A: Found. Crystallogr. 47* (part 2), 110−119.

27. Otwinowski, Z., and Minor, W. (1997) Processing of X-ray diffraction data collected in oscillation mode, *Methods Enzymol. 276*, 307−326.
28. CCP4 (1994) The CCP4 suite: Programs for X-ray crystallography, *Acta Crystallogr., Sect. D: Biol. Crystallogr. 50*, 760−763.
29. Brunger, A. T., Adams, P. D., Clore, G. M., DeLano, W. L., Gros, P., Grosse-Kunstleve, R. W., Jiang, J. S., Kuszewski, J., Nilges, M., Pannu, N. S., Read, R. J., Rice, L. M., Simonson, T., and Warren, G. L. (1998) Crystallography and NMR system: A new software suite for macromolecular structure determination, *Acta Crystallogr., Sect. D: Biol. Crystallogr. 54* (part 5), 905−921.
30. Flanagan, J. G., and Vanderhaeghen, P. (1998) The ephrins and Eph receptors in neural development, *Annu. Rev. Neurosci. 21*, 309−345.
31. Koolpe, M., Dail, M., and Pasquale, E. B. (2002) An ephrin mimetic peptide that selectively targets the EphA2, *J. Biol. Chem. 277*, 46974−46979.
32. Murai, K. K., Nguyen, L. N., Koolpe, M., McLennen, R., Krull, C. E., and Pasquale, E. B. (2003) Targeting the EphA4 receptor in the nervous system with biologically active peptides, *Mol. Cell. Neurosci. 24*, 1000−1011.
33. Stein, E., Lane, A. A., Cerretti, D. P., Schoecklmann, H. O., Schroff, A. D., van Etten, R. L., and Daniel, T. O. (1998) Eph receptors discriminate specific ligand oligomers to determine alternative signaling complexes, attachment, and assembly responses, *Genes Dev. 12*, 667−678.
34. Wieland, I., Jakubiczka, S., Muschke, P., Cohen, M., Thiele, H., Gerlach, K. L., Adams, R. H., and Wieacker, P. (2004) Mutations of the ephrin-B1 gene cause craniofrontonasal syndrome, *Am. J. Hum. Genet. 74*, 1209−1215.
35. Twigg, S. R., Kan, R., Babbs, C., Bochukova, E. G., Robertson, S. P., Wall, S. A., Morriss-Kay, G. M., and Wilkie, A. O. (2004) Mutations of ephrin-B1 (EFNB1), a marker of tissue boundary formation, cause craniofrontonasal syndrome, *Proc. Natl. Acad. Sci. U.S.A. 101*, 8652−8657.
36. Day, B., To, C., Himanen, J. P., Smith, F. M., Nikolov, D. B., Boyd, A. W., and Lackmann, M. (2005) Three distinct molecular surfaces in ephrin-A5 are essential for a functional interaction with EphA3, *J. Biol. Chem. 280*, 26526−26532.

BI050789W